Available online at www.sciencedirect.com
ScienceDirect
Journal of Power Sources 164 (2007) 572–577
JOURNAL OF POWER SOURCES
www.elsevier.com/locate/jpowsour

Short communication

A novel non-noble electrocatalyst for oxygen reduction in proton exchange membrane fuel cells

Hexiang Zhong [a,b], Huamin Zhang [a,*], Yongmin Liang [a,b], Jianlu Zhang [c], Meiri Wang [a], Xiaoli Wang [a,b]

[a] *Proton Exchange Membrane Fuel Cell Key Materials and Technology Laboratory, Dalian Institute of Chemical Physics, Chinese Academy of Sciences, P.O. Box 110, Dalian 116023, China*
[b] *Graduate School of the Chinese Academy of Sciences, Beijing 100039, China*
[c] *Institute for Fuel Cell Innovation, National Research Council Canada, Vancouver, BC, Canada V6T 1W5*

Received 20 October 2006; received in revised form 15 November 2006; accepted 16 November 2006

Abstract

Tungsten nitride supported on carbon black was prepared by temperature-programmed reaction (TPR) process and is proposed as a catalyst for the oxygen reduction reaction (ORR) in proton exchange membrane fuel cells (PEMFCs). The as-prepared catalyst was characterized by X-ray diffraction (XRD) and transmission electron microscopy (TEM) techniques. The ORR activities of the catalyst were studied by electrochemical measurements and single cell tests, respectively. The results indicated that the tungsten nitride electrocatalyst exhibited attractive catalytic activity and stability for the ORR in PEMFCs. It is expected to be a promising cathode electrocatalyst for PEMFCs, especially for the comparatively high temperature proton exchange membrane fuel cells.

Keywords: PEMFCs; Tungsten nitride; Oxygen reduction reaction; Non-noble catalysts

1. Introduction

Platinum supported on electron-conductive carbon black has hitherto been widely used as the oxygen reduction reaction (ORR) catalyst since it has been generally recognized as the most active and stable catalyst for the ORR in proton exchange membrane fuel cells (PEMFCs). However, the scarce resources and the high cost of platinum hamper the commercialization of PEMFCs. To reduce the cost of the Pt catalysts, two approaches have been adopted: exploring non-noble catalysts and reducing the Pt loading [1,2]. Alloying Pt with other metals (Fe, Co, Ni, Cu, etc.) is one effective approach pursued to reduce the Pt loading and to lower the cost of the electrocatalysts. However, the non-noble metals in the Pt alloys are usually easily dissolved in the acid media and at the high potentials in PEMFCs. As for the approach using non-noble catalysts, several candidates, such as transition metal chalcogenides [3,4], transition metal oxides [5], macrocycles (porphyrin or phthalocyanine) whether heat treated or not [6,7] and so on, have been proposed over the years for cathode electrocatalysts.

Since Boudart and Levy [8] reported the platinum-like properties of tungsten carbide (WC) for H_2–O_2 titration, carbides and nitrides were intensively investigated for their suitability as a promising substitution for platinum electrocatalysts in PEMFCs [9–11]. Yang et al. [11] investigated the electrocatalytic activities of tungsten carbide based carbides as the electrocatalysts for hydrogen oxidation in PEMFCs. Palanker et al. [12] reported that CO was inert on WC. Attempts have also been made to utilize carbides- and nitride-based catalysts in the ORR [13,14]. TiN has been investigated as the ORR electrocatalyst in alkaline solution [15] and molybdenum nitride has been studied in acid solution and PEMFCs [16]. However, there are no data in the literature regarding the electrode performance of tungsten nitride as the primary cathode catalyst material in PEMFCs. In this paper, we presented a novel electrocatalyst, tungsten nitride supported on carbon black, for the ORR in PEMFCs. The presence of nanosized tungsten nitride was confirmed by X-ray diffraction (XRD) and transmission electron microscopy

* Corresponding author. Tel.: +86 411 84379072; fax: +86 411 84665057.
E-mail address: Zhanghm@dicp.ac.cn (H. Zhang).

0378-7753/$ – see front matter © 2006 Elsevier B.V. All rights reserved.
doi:10.1016/j.jpowsour.2006.11.080

(TEM). And the ORR activities of the catalyst were assessed by electrochemical measurements and single PEMFC tests. The stability of the catalyst was also investigated in the single cell test.

2. Experimental

2.1. Catalyst preparation

The catalyst, tungsten nitride supported on carbon black (Vulcan XC-72R, Cabot Corp., BET: 237 $m^2\,g^{-1}$, USA, denoted as C) with 18 wt.% of the tungsten content, was prepared by temperature-programmed reaction (TPR) process as described in literature [16]. The preparation process of the catalyst was composed of two steps: the preparation of the precursor oxide and the nitrification of the precursor. The first step was the preparation of the precursor oxide by the incipient wetness method as follows.

Firstly, XC-72R carbon black was impregnated using the incipient wetness method with the required amount of ammonium metal tungstate dissolved in a mixture of water and the dispersing agent. After impregnation for 12 h, the sample was agitated and dried in a water bath at 80 °C until the water had evaporated, and subsequently transferred into an oven to dry at 120 °C overnight. Finally, it was calcined for 2 h at 500 °C in a quartz tube furnace under N_2 atmosphere to obtain the precursor of W_2N/C.

The precursor was then nitrified under flowing NH_3 atmosphere using the following TPR process: the temperature was firstly increased to 350 °C at a rate of 5 °C min^{-1}, then to 450 °C by 0.5 °C min^{-1} and to 750 °C by 2.5 °C min^{-1} and finally the temperature maintained at 750 °C for 2 h. When the reaction was over, the sample was cooled to room temperature under nitrogen atmosphere and the catalyst W_2N/C (18 wt.% W) was thus obtained.

2.2. Physical characterizations

XRD analysis of the W_2N/C (18 wt.% W) catalyst was carried out on a PANalytical X'Pert PRO diffractometer (Philips X'Pert PRO) using a Ni-filtered Cu Kα source (λ = 1.54056 Å) to characterize the crystalline structure of the as-prepared catalyst powder. The 2θ values of X-ray diffractograms varied between 20° and 95° with a step size of 0.017°, accumulating data for 8.255 s per step. A transmission electron microscopy image of W_2N/C (18 wt.% W) was recorded on a JEOL JEM-2000EX microscope operated at 100 kV. A sample for TEM measurement was prepared by ultrasonically suspending the catalyst powder in ethanol and then placing a drop of the suspension on an amorphous carbon film on a Cu grid. Particle size distributions for the catalysts were obtained by manually measuring 200 particles. The mean particle diameter (D_m) was calculated by the following formula [17]:

$$D_m = \frac{\sum_i n_i d_i}{\sum_i n_i}$$

2.3. Electrochemical characterizations

The linear scan voltammetry (LSV) measurements were carried out using an EG&G potentiostat/galvanostat Model 263A (Princeton Applied Research) and a standard three-electrode test cell at room temperature. The working electrode was a thin layer of Nafion® bonded catalyst inks cast on a carbon rotating disk electrode. A Pt foil and a saturated calomel electrode (SCE) were used as the counter and reference electrode, respectively. However, all potentials in the article were quoted to the standard hydrogen electrode (SHE) in the same solution, unless stated otherwise. The measurements were conducted in a 0.5 M H_2SO_4 solution. Ultra-pure oxygen or nitrogen was bubbled into the 0.5 M H_2SO_4 to maintain an oxygen or oxygen-free atmosphere near the working electrode. The glass carbon (GC) electrode was polished with 0.05 μm alumina slurries. After polishing, the electrode was washed in ethanol in an ultrasonic bath and then dried under vacuum. The electrode was subsequently washed carefully with triple distilled water, just before placing it in the cell for electrochemical measurement. The thin film on the GC electrode was prepared as follows: 10 mg W_2N/C catalyst and 1.0 mL ethanol and 80 μL 5% Nafion® solution (Du Pont, USA) were mixed and ultrasonicated about 30 min to form a homogeneous black ink. And then a 25 μL aliquot of this ink was cast on the GC electrode surface. And the platinum supported on the carbon black (20 wt.%, Johnson Matthey) was measured under the same condition as the comparison. The LSV curves were obtained in the potential range of 1.1–0.1 V versus SHE with a scan rate of 5 mV S^{-1}.

2.4. Preparation of membrane electrode assembly and single cell tests

The single cell tests were conducted with a 5 cm^2 membrane electrode assembly (MEA) using W_2N/C (18 wt.% W) as the cathode electrocatalyst. In all experiments reported in this paper, Nafion®-1035 (Du Pont) was used as the membrane. The 46.2 wt.% Pt/C catalyst (TKK) was used as the anode catalyst and the Pt loading of anode was 0.3 mg cm^{-2}. The catalyst was mixed with appropriate amount of isopropanol and 5% Nafion® solution suspension (W_2N/C:Nafion® = 2:1 by dried weight) and ultrasonicated to form an ink-like slurry. The slurry was then cast onto a prefabricated gas diffusion layer (SGL carbon paper as substrate, 40 wt.% PTFE) and heat-treated at 130 °C for 30 min in a vacuum oven to obtain the cathode electrode. The Nafion®-1035 membranes were pretreated before use by the following procedure: the membranes were boiled in 3% H_2O_2 solution and then in 0.5 M H_2SO_4 to remove organic and mineral impurities, respectively. And then they were rinsed several times with hot distilled water. The treated membrane was sandwiched between two gas diffusion layers followed by a hot-pressing procedure at 140 °C and 10 MPa for 1 min to form a membrane electrode assembly. Fuel cell polarization measurements were carried out at different temperatures. The fuel (H_2) and the oxidant (O_2) were humidified by passing them through water bathes at temperatures of 90 °C and 85 °C, respectively. The gas pressures were all kept at 0.2 MPa at both electrodes. Performance data

were recorded in the steady state and the polarization curves were uncorrected for internal resistance losses. The stability test of the catalyst was also carried out under the same conditions.

2.5. Electrochemical impedance spectra

The electrochemical impedance spectra (EIS) of the single cells were recorded using an EG&G Model 1025 Solartron frequency response analyser and Model 263A potentiostat/galvanostat (EG&G Instruments Corp.). The amplitude of the sinusoidal modulation voltage was 10 mV. The anodes of the single cells were used as the reference electrode and counter electrode, respectively. The cathodes were used as the working electrode, respectively. The impedance spectra of single cells in the high frequency range show inductive behavior, characteristic to the experimental setup. Such inductive characteristics have been reported by other researchers in impedance studies on batteries and fuel cells [18]. To avoid complications resulting from these characteristics, we limited the high-frequency range to 1 kHz. And the low-frequency range was 100 mHz.

3. Results and discussion

3.1. Characterizations of the electrocatalyst

X-ray diffraction was performed to obtain structural information of the catalyst. As shown in Fig. 1, the XRD pattern for the tungsten nitride exhibits characteristic diffraction peaks corresponding to a single-phase fcc structure of β-W_2N nanocrystals [19] and the Vulcan XC-72R support. In addition, XRD pattern shows the (1 1 1) diffraction line to be the preferred orientation where adatom mobilities are sufficiently high to favor crystallites bounded by low energy planes. This indicated that the W metal is not contained in the catalyst, which can cause the change of the main peak [20]. The average crystallite size of the β-W_2N in the catalyst, calculated by using the Scherrer formula from the peak (1 1 1) of β-W_2N, is about 4 nm.

Fig. 2(a) shows the TEM image of the W_2N/C catalyst. Fig. 2(b) shows the particle size distribution obtained from

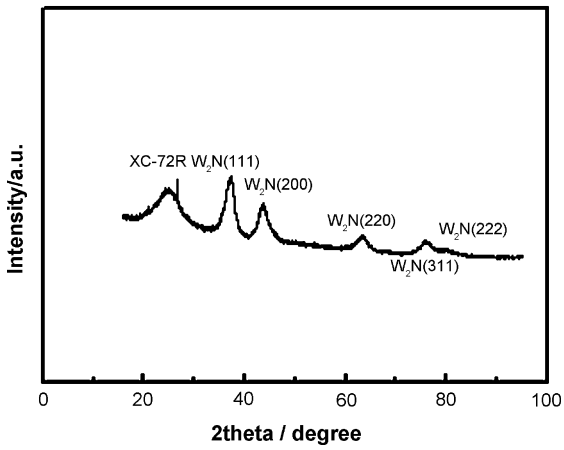

Fig. 1. X-ray diffraction pattern of the W_2N/C (18 wt. % W).

Fig. 2(a). As shown in the TEM image, most of the catalyst nanoparticles are dispersed homogenously as small and uniform spots over the surface of the carbon support. The size distribution peak ranges between 2.5 nm and 7 nm and the average crystallite diameter is about 4 nm. This result is consistent with particle size measured by the XRD. Some of the larger particles appear to be agglomerates of several smaller ones due to the calcination at high temperature during the preparation of the catalyst.

3.2. Electrochemical properties

The LSV curves were measured in N_2 and O_2 saturated solutions, respectively, to investigate the ORR activity of the W_2N/C (18 wt.% W) catalyst in 0.5 M H_2SO_4. And the activity of commercial Pt/C (Johnson Matthey) under O_2 atmosphere was also investigated as the comparison. As shown in Fig. 3, almost no apparent reduction current is observed in the potential range for the W_2N/C catalyst under N_2 atmosphere, which demonstrates the high stability of the as-prepared tungsten nitride catalyst in the N_2 atmosphere. On the other hand, the reduction currents of the tungsten nitride and Pt/C in O_2 saturated solution significantly increase with the potential scanning. The apparent difference between the two cases indicates that the W_2N/C cata-

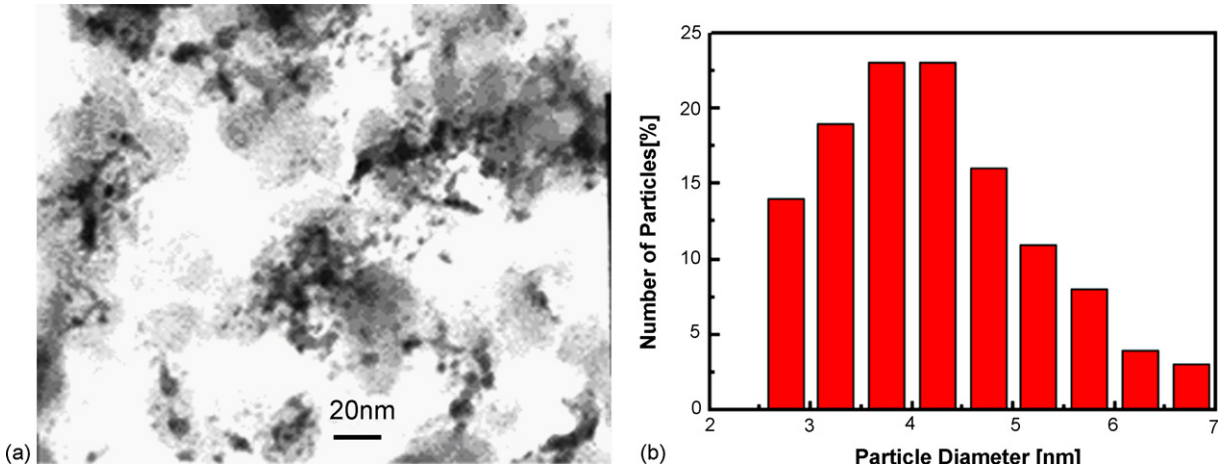

Fig. 2. TEM analysis of W_2N/C (18 wt.%) catalyst with 300,000 magnifications. (a) TEM image and (b) corresponding particle size distribution.

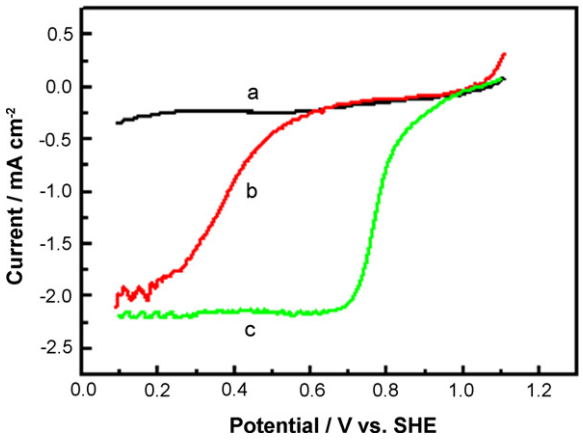

Fig. 3. Linear scan voltammograms for different catalysts in 0.5 M H_2SO_4 solution. (a) W_2N/C (43 mg W_2N) in the 0.5 M H_2SO_4 solution saturated with nitrogen; (b) W_2N/C (43 mg W_2N) in the 0.5 M H_2SO_4 solution saturated with oxygen; (c) Pt/C (12 mg Pt) in the 0.5 M H_2SO_4 solution saturated with oxygen. Scan rate = 5 mV s^{-1}, 25 °C.

lyst has good electrocatalytic activity for the ORR. And we also can see that the ORR on the electrode modified by the W_2N/C catalyst starts at a relatively positive potential as a non-noble catalyst, about 0.6 V, although it is still negative than that of Pt/C. The comparatively high ORR activity of the as-prepared catalyst is considered to be attributed to the synergistic effect between the W and N [21], as well as the nanostructure, which is capable of providing highly active sites [22].

3.3. Single cell tests

Fig. 4 shows the performances of the single cell achieved at different temperatures, from 60 °C to 80 °C, with the as-prepared W_2N/C (18 wt.% W) as the cathode electrocatalyst. The loading of the catalyst is 0.644 mg cm^{-2}. As illustrated in Fig. 4, the W_2N/C exhibits relatively good performance and the improvement of the performances is also observed as the temperature increased. At the current density of 100 mA cm^{-2}, the cell voltage at 80 °C is 0.367 V, which is about 146 mV and 223 mV higher than that at 70 °C and 60 °C, respectively. And the maximum power densities of the single cells are 16.02 mW cm^{-2}, 24.4 mW cm^{-2} and 39.2 mW cm^{-2} from 60 °C to 80 °C, respectively. This behavior is indicative of an enhancement to the electrocatalytic kinetic reduction of the adsorbed oxygen with the increase of temperature.

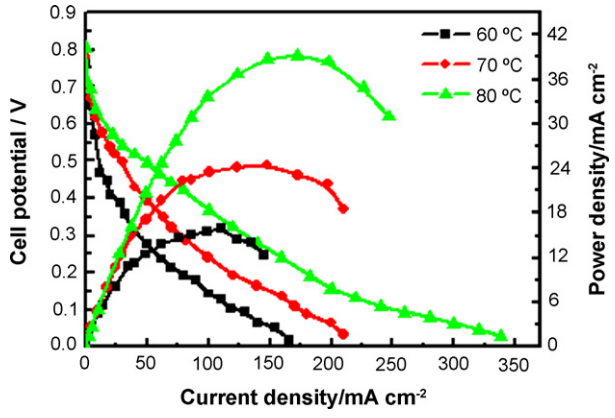

Fig. 4. Polarization curves at different cell temperatures of the single cell with the W_2N/C (18 wt.% W) as the cathode catalyst.

3.4. EIS measurements

The EIS spectra at different temperatures obtained for the single cell with W_2N/C (18 wt.% W) as the cathode electrocatalyst are shown in Fig. 5(a). The EIS measurements are conducted at a constant current 100 mA cm^{-2}. It is found from the spectra that the semicircle is made of two high frequency (HF) capacitive loops, small loop (usually not apparent) at the highest frequency (HF) end overlapped by a large arc at the middle high frequency (MHF). It is supposed that this HF loop is due either to the ionic ohmic drop/double layer charging inside the active layer in the granular electrode structure, or to electronic contact problems between the electronic supply and the GDE gas diffusion layer (RC parallel equivalent circuit) [23,24]. In our experiment, the high frequency arc is more distinct than that reported in the literature, and it is suspected due to the thick catalyst layer of the electrode prepared by conventional method in the experiment and the low loading of tungsten nitride. Especially at low current densities, there is insufficient water in the granular electrode structure, the agglomerates contract, so the grain boundary resistance increases, resulting in a thinner and longer path for the migration of ions, increasing the ionic ohmic resistance and capacitances [25,26]. Then, we may conclude that if the thickness of the catalyst layer of the electrode is decreased, the high frequency arc may not be as distinct as observed in the ac impedance spectra. The large loop at intermediate frequencies is attributed to the charge transfer resistance and the double

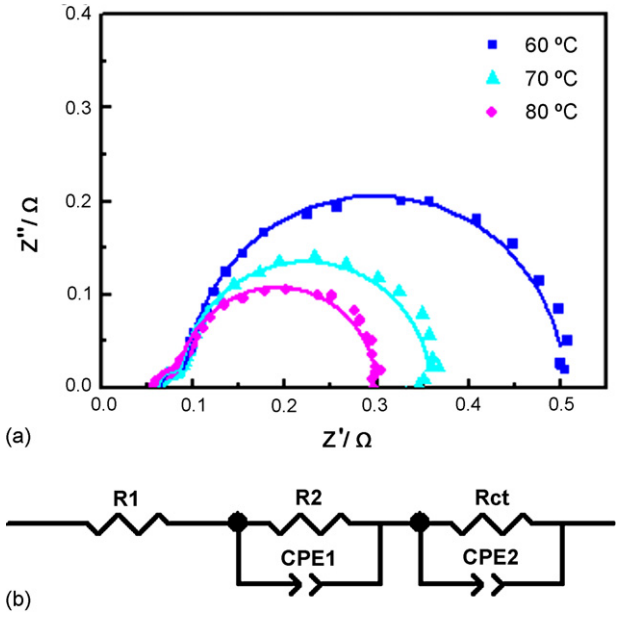

Fig. 5. (a) EIS of PEM single cell at different cell temperatures with the as-prepared catalyst as the cathode catalyst anode humidifier temperature 90 °C, cathode humidifier temperature 85 °C; pressure 0.2 MPa/0.2 MPa. Legend specifies temperature of the experiment. (b) Equivalent circuit for the single cell.

Table 1
Parameters evaluated from fit of EIS with the equivalent circuit shown in Fig. 5(b)

Temperature (°C)	R_1 (Ω)	R_2 (Ω)	R_{ct} (Ω)
60	0.0665	0.02681	0.4109
70	0.0634	0.02495	0.2711
80	0.0621	0.02476	0.2149

layer capacity and the relaxations of the intermediate species [27,28].

An equivalent circuit was constructed to describe the process, as shown in Fig. 5(b). R_1 represents the impedance at the intersection of the HF curve with the real axis. It is attributed to the internal resistance of the cell including the total ohmic resistance of the cell, which can be expressed as a sum of the contributions from uncompensated contact resistance and ohmic resistance of the cell components such as membrane, catalyst layer, backing, end plate, and that between each of them [26]. R_2 and CPE_1 represent the resistance and constant phase element at the HF small loop, which relates to electrode structure. R_{ct} is the charge-transfer resistance for oxygen reduction, and CPE_2 constant phase element represents the R_{ct} associated catalyst layer capacitance properties.

Table 1 shows the simulated data using the equivalent circuit in Fig. 5(b) by ZView. It can be seen that, as expected, R_2 decreases from 26.81 mΩ to 24.76 mΩ when the temperature increases from 60 °C to 80 °C. It is supposed that the membrane is well hydrated by the water produced in the cell reaction with the increase of the temperature, which contributes to the change of the properties of the electrode structure and in result affects the R_2. And the charge-transfer resistance R_{ct} decreases from 410.9 mΩ to 214.9 mΩ. This demonstrates that the charge transfer resistance greatly decreases and confirms the increased cell performance with the temperature increased. And the charge transfer resistance R_{ct} of the single cell at 80 °C is about 214.9 mΩ, which is higher than that of Pt/C MEAs [26,28]. In addition, the internal resistance of the cell decreases with temperature, which is also higher than that of normal Pt/C MEAs in the same fixture [29]. It is caused by the thick catalyst layer of the electrode and the properties of the catalysts itself. The high charge transfer resistance and the high internal resistance are major factors contributing to the reduced *V–I* performance of the present cell compared to the Pt/C catalyst.

3.5. Stability test

Stability test for the W_2N/C electrocatalyst was carried out at the current density of 120 mA cm^{-2} under fuel cell conditions. The single cell output voltage was recorded versus the test time. According to the results illustrated in Fig. 6, it was found that the single cell output voltage maintains almost at the same value during the test time; there was no obvious performance degradation under fuel cell conditions. The high stability of the catalyst may be due to the high stability of the tungsten nitride itself in low potential and some oxides of WO_2 on the surface maybe also increase the activity and the stability of the catalyst [30].

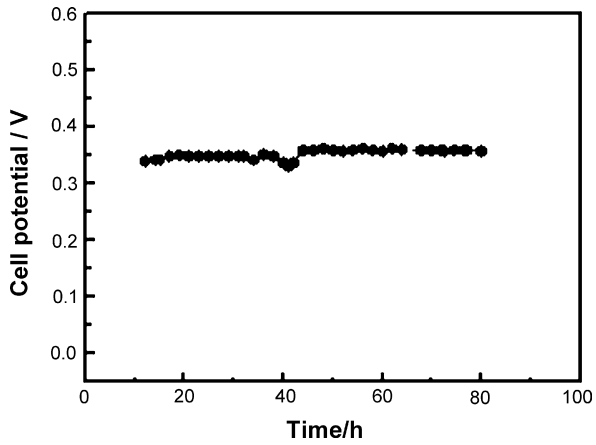

Fig. 6. Stability test of the as-prepared catalyst at the constant current density.

4. Conclusions

A new non-noble electrocatalyst for PEMFCs based on tungsten nitride was prepared by a TPR process and tested for the electroreduction of oxygen. The catalyst exhibited comparatively good activity for the ORR in both acid solutions and PEM fuel cells. And the electrocatalytic kinetic reduction of the adsorbed oxygen can be enhanced as the temperature increased. Furthermore, the catalyst showed good stability in real single cell tests. Although the activity of the W_2N/C toward ORR is inferior to that of the commercially available Pt/C catalysts widely used in PEMFCs, it is a novel non-noble catalyst material, which shows comparatively high activity among non-noble cathode electrocatalysts in PEMFCs [31–33]. We believe that further optimizations in both the catalyst preparation process and MEA manufacture could enhance the activity of the catalyst toward the ORR. And probably we also can improve the operational temperature of the single cells to enhance the activity of the catalyst. Thus, the comparatively high temperature proton exchange membrane fuel cells may be also a potential field for the catalyst. Further refinement of the preparative conditions for the catalyst is under way.

Acknowledgement

This work was financially supported by National Natural Science Foundation of China (Grant No. 50236010).

References

[1] S. Ye, A. Vijh, L. Dao, J. Electroanal. Chem. 415 (1996) 115–121.
[2] L. Zhang, J. Zhang, D.P. Wilkinson, H.J. Wang, J. Power Sources 156 (2005) 171–182.
[3] N. Alonso-Vante, H. Tributsch, Nature 323 (1986) 431–432.
[4] N. Alonso-Vante, W. Jaegermann, H. Tributsch, W. Honle, K. Yvon, J. Am. Chem. Soc. 109 (1987) 3251–3257.
[5] R.W. Reeve, P.A. Christensen, A.J. Dickinson, A. Hamnett, K. Scott, Electrochim. Acta 145 (2000) 3463–3471.
[6] M.C. Martins Alves, J.P. Melet, D. Guay, M. Ladouceur, G. Tourillon, J. Phys. Chem. 96 (1992) 10898–10905.
[7] L.T. Weng, P. Bertrand, G. Lalande, D. Guay, J.P. Dodelet, Appl. Surf. Sci. 84 (1995) 9–21.
[8] M. Boudart, R.B. Levy, Science 181 (1973) 547–549.

[9] S.T. Oyama, J.C. Schlatter, J.E. Metcalfe, J.M. Lambert, Ind. Eng. Chem. Res. 27 (1988) 1639–1653.
[10] R. Venkataraman, H.R. Kunz, J.M. Fenton, J. Electrochem. Soc. 150 (2003) A278–A284.
[11] X.G. Yang, C.Y. Wang, Appl. Phys. Lett. 86 (2005) 224104–224107.
[12] V.S. Palanker, R.A. Gajyev, D.V. Sokolsky, Electrochim. Acta 22 (1977) 133–136.
[13] K. Lee, A. Ishihara, S. Mitsushima, N. Kamiya, K. Ota, Electrochim. Acta 49 (2004) 3479–3485.
[14] H. Meng, P.K. Shen, Electrochem. Commun. 8 (2006) 588–594.
[15] F. Mazza, S. Trassatti, J. Electrochem. Soc. 110 (1963) 847–848.
[16] H.X. Zhong, H.M. Zhang, G. Liu, Y.M. Liang, J.W. Hu, B.L. Yi, Electrochem. Commun. 8 (2006) 707–712.
[17] Y. Liang, H. Zhang, H.X. Zhong, X.B. Zhu, Z.Q. Tian, D.Y. Xu, B. Yi, J. Catal. 238 (2006) 468–476.
[18] J.P. Dirard, B. Le Gorec, P. Landaud, C. Montella, Electrochim. Acta 42 (1997) 3417–3420.
[19] Y.G. Shen, Y.W. Mai, Appl. Surf. Sci. 167 (2000) 59–68.
[20] Y.G. Shen, Y.W. Mai, W.E. McBride, Q.C. Zhang, D.R. McKenzie, Thin Solid Films 372 (2000) 257–264.
[21] G. Soto, W. de la Cruz, F.F. Castillo'n, J.A. Di'az, R. Machorro, M.H. Fari'as, Appl. Surf. Sci. 214 (2003) 58–67.
[22] R.C.V. McGee, S.K. Bej, L.T. Thompson, Appl. Catal. A 284 (2005) 139–146.
[23] O. Antoine, Y. Bultel, R. Durand, P. Ozil, Electrochim. Acta 43 (1998) 3681–3691.
[24] M. Ciureanu, R. Roberge, J. Phys. Chem. B 105 (2001) 3531–3539.
[25] V.A. Paganin, C.L.F. Oliveria, E.A. Ticianilli, T.E. Springer, E.R. Gonzalez, Electrochim. Acta 43 (1998) 3761–3766.
[26] F.Q. Liu, B.L. Yi, D.M. Xing, J.R. Yu, Z.J. Hou, Y.Z. Fu, J. Power Sources 124 (2003) 81–89.
[27] C. Fischer, N. Alonso-Vante, S. Fiechter, H. Tributsch, J. Appl. Electrochem. 25 (1995) 1004–1008.
[28] B. Andreaus, G.G. Scherer, Solid State Ionics 168 (2004) 311–320.
[29] O. Antoine, Y. Bultel, R. Durand, J. Electroanal. Chem. 499 (2001) 85–94.
[30] H. Okamoto, G. Kawamuro, A. Ishikawa, T. Kudo, J. Electrochem. Soc. 134 (1987) 1649–1653.
[31] R. Manoharan, J.B. Goodenough, Electrochim. Acta 40 (1995) 303–307.
[32] R.L. Bradford, J.S. Ronald, A.J. Turner, Electrochim. Acta 50 (2005) 1169–1179.
[33] R.G. Gonz'alez-Huerta, J.A. Ch'avez-Carvayar, O. Solorza-Feria, J. Power Sources 153 (2006) 11–17.